Annals of Biomedical Engineering, Vol. 24, pp. 37–47, 1996
Printed in the USA.

0090-6964/96 $10.50 + .00

Chaotic Oscillations in Microvessel Arterial Networks

SILVIO CAVALCANTI and MAURO URSINO

Department of Electronics, Computer Science and Systems, University of Bologna, Bologna, Italy

Abstract—A mathematical model of a multibranched microvascular network was used to study the mechanisms underlying irregular oscillations (vasomotion) observed in arteriolar microvessels. The network's layout included three distinct terminal arteriolar branches originating from a common parent arteriole. The biomechanical model of the single microvessel was constructed to reproduce the time pattern of the passive and active (myogenic) response of arterioles in the hamster cheek pouch to a step-wise arterial pressure change. Simulation results indicate that, as a consequence of the myogenic reflex, each arteriole may behave as an autonomous oscillator, provided its intraluminal pressure lies within a specific range. In the simulated network, the interaction among the various oscillators gave rise to a complex behavior with many different oscillatory patterns. Analysis of model bifurcations, performed with respect to the arterial pressure level, indicated that modest changes in this parameter caused the network to shift between periodic, quasiperiodic, and chaotic behavior. When arterial pressure was changed from approximately 60–150 mm Hg, the model exhibited a classic route toward chaos, as in the Ruelle-Takens scenario. This work reveals that the nonlinear myogenic mechanism is able to produce the multitude of different oscillatory patterns observed *in vivo* in microvascular beds, and that irregular microvascular fluctuations may be regarded as a form of deterministic chaos.

Keywords—Vasomotion, Chaos, Nonlinear dynamics, Myogenic reflex, microvascular networks.

INTRODUCTION

Arterial microvessels frequently exhibit a spontaneous, rhythmic activity, called vasomotion, that appears as an oscillation in vessel lumen and in blood flow. Vasomotion has been revealed in several microcirculatory studies both in isolated arterioles and in whole terminal vascular beds (7,19,27). It seems that this phenomenon is not restricted to specific peripheral vascular districts, but rather it is believed to be a characteristic of most microcirculation vessels, *i.e.*, vessels with diameters ranging between 5 and 50 μm.

The rhythmic vasomotor activity of microvessels arises, of course, from their contractile capacity, but the genesis of vascular oscillations has different explanations. One reliable hypothesis imputes vasomotion to the action of the local mechanisms controlling microvessel lumen. Stress- and metabolic-dependent mechanisms, which contribute to setting the vascular muscle tone, behave like nonlinear feedbacks that, under certain conditions, may induce the microvessel to oscillate. In particular, arterioles exhibit a pressure-dependent active response known as the myogenic reflex (3): The increase of vascular wall tension caused by a rise in blood pressure intensifies the smooth muscle activity, thereby eliciting a sustained vessel constriction. The myogenic reflex operates as a local control mechanism that contributes to maintaining a constant blood flow through the peripheral circulation, despite large pressure variations. A mathematical analysis of microvessel regulatory processes demonstrated that the myogenic control may cause biomechanical instability and vessel lumen oscillations (29).

Vasomotion is known to be affected by several physical factors, such as vessel size, magnitude of transmural pressure, flow velocity, etc. Under the influence of these factors, microvessels exhibit complex behavior. Within the same vascular bed, one can simultaneously observe active vessels and apparently inert arterioles, characterized by no change in diameter. Moreover, owing to some trigger perturbation, inert vessels may begin to oscillate, and the active ones may settle down. Oscillations occurring in different branches of the arteriolar network propagate along the vascular bed and mutually interplay, producing both simple and complex time patterns. Sometimes, vessel oscillations seem to be synchronized, with a well-defined periodic pattern and a common frequency within the range of 1–20 cycles min^{-1} (7). More often, oscillation coupling generates new subhormone and superharmonic rhythms or quasiperiodic oscillations. Finally, it is possible to observe vessels presenting irregular, aperiodic luminal changes (5,7). In this case, vessel diameter exhibits unpredictable fluctuations with an apparent stochastic nature and no time correlation. The frequency analysis of such complex oscillations reveals a broad power spectrum, with superimposed peaks indicating some predominant rhythms (7,19). The analysis of *in vivo* time series of such irregular diameter oscillations (16,30) suggested that apparently random fluctuations actually may be deterministic in origin.

Address correspondence to S. Cavalcanti, D.E.I.S., Viale Risorgimento, 2, I-40136 Bologna, Italy.

(Received 25May95, Revised, Revised, Accepted 8Aug95)

The wealth of different kinds of behavior, including the erratic, apparently random time fluctuations, and the sensitivity to experimental conditions reveal the typical scenario of a phenomenon that is chaotic in nature. In this study, we investigated this aspect of vasomotion and paid specific attention to the role that the myogenic control of microvessel lumen plays in the phenomenon. Previous mathematical analyses (1,13,29) provided a convincing theoretical framework for the possible origin of periodic diameter changes in muscular vessels and noted that the myogenic mechanism was implicated in the genesis of self-sustained vessel oscillations. None of these works, however, predicted the presence of more complex patterns, such as aperiodic or chaotic fluctuations, or examined the role of vasomotion in the presence of multiple microvessel branching. To overcome these limitations, a novel mathematical model of a microvessel network, including branching and the arteriolar myogenic regulation, is presented herein. The model is able to reproduce vessel oscillations with time patterns similar to those observed during *in vivo* microvascular studies. Model simulations suggest that nonlinear interaction between oscillations arising in distinct points of the network may be the cause of periodic, as well as aperiodic, time evolutions.

METHODS

Mathematical Model of the Single Arteriole

The biomechanical model of the pressure-dependent diameter changes was derived by distinguishing the passive, viscoelastic response of the arterial wall from the active response caused by the myogenic reflex. In particular, the viscoelastic properties of the arteriolar wall in a purely passive state were assumed not to be influenced by the active myogenic vasoconstriction. Under this assumption, the vessel diameter was expressed as the sum of a elastic deformation, d_e, and a myogenic contraction, d_m,

$$d(p) = d_e(p) + d_m(p) \tag{1}$$

where p denotes the intraluminal pressure. Vessel diameter changes in response to rapid pressure elevations consisted of both static and dynamic components, which were modeled separately, as presented below.

Steady-State Characteristics. Under the steady-state condition, the arteriole elastic deformation exhibited a typical exponential behavior: wall material appeared to be soft at low pressures and became more rigid as pressure increases (Fig. 1). To reproduce this behavior, the elastic deformation in the passive state was assumed to depend on pressure according to the following expression:

$$\tilde{d}_e(p) = d_o + g\,p + \delta(1 - e^{-\gamma p}) \tag{2}$$

where the tilde ($\simeq$) denotes the steady condition and d_o is the undeformed vessel diameter ($p = 0$).

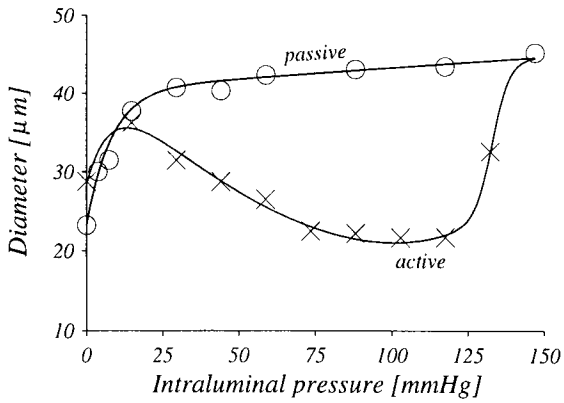

FIGURE 1. Steady-state pressure-diameter relationships measured by Davis and Sikes (10) in a second order arteriole of the hamster cheek pouch *in vitro*, first in a passive state (Ca^{2+} free solution) (○) and then in active state (physiological solution) (×). Solid lines represent model simulations of the same responses computed by Eqs. 1 through 3 (parameter values are listed in the first column of Table 1).

When the myogenic reflex was active, the arteriolar deformation was appreciably different from the passive case (Fig. 1). At low pressure elastic deformation prevailed on the myogenic contraction, and the steady-state pressure-diameter curve was very close to the passive one. As pressure increased, the vessel became stiffer, the elastic dilatation was smaller than the myogenic contraction, and the characteristic exhibited a segment with negative slope, denoting the myogenic range of the arteriole. For high values of pressure, the myogenic response falls, and the vessel deformation tends to the elastic characteristic again. To reproduce this behavior, the active steady-state contraction was modeled through an empirical expression

$$\tilde{d}_m(p) = \frac{a - \sqrt{b + cp}}{1 + f_1 e^{\alpha p} + f_2 e^{\beta p}} \tag{3}$$

A value was assigned to parameters of the elastic (2) and myogenic (3) characteristics (Table 1) in order to best fit the pressure-diameter data obtained in steady-state conditions in isolated arterioles of the hamster cheek pouch circulation (8–10). These data were obtained either after chemical inactivation of the myogenic response, which corresponded to the purely elastic state, or when the myogenic reflex was active (Fig. 1).

Dynamic Responses. The dynamic response to intraluminal pressure changes was derived by assuming that the inertial effect caused by the wall mass was negligible and by taking into consideration only the viscous force caused by the wall motion. The dynamics of elastic deformation, therefore, was described by the differential equation

$$\dot{d}_e(t) = \frac{1}{\tau_e(t)}\,(\tilde{d}_e(p) - d_e), \text{ with } \tau_e(t) = \tau_{eoe} - \mu\dot{p}(t). \tag{4}$$

TABLE 1.

	Elastic	
	R_i	R_s, R_m, R_i
d_o (μm)	23.23	6.24
g (μm mm Hg^{-1})	2.85×10^{-2}	4.02×10^{-2}
δ (μm)	17.2	15.6
γ (mm Hg^{-1})	0.12	0.19
τ_{eo} (sec)	2	2
μ (sec mm Hg^{-1})	1.24×10^{-2}	1.24×10^{-2}
	Myogenic	
a (μm)	23.23	21.12
b (μm^2)	327.27	270.48
c (μm^2 mm Hg^{-1})	22.81	29.23
f_1	0.01	0.01
α (mm Hg^{-1})	3.24×10^{-2}	5.02×10^{-2}
f_2	5.13×10^{-22}	5.13×10^{-22}
β (mm Hg^{-1})	0.37	0.58
τ_{mo} (sec)	10	4
t_d (sec)	6	3 (R_s) 3.5 (R_m) 4 (R_i)

The mechanical equivalent of this equation is the Kelvin-Voigt model (see 11), which has a nonlinear spring coupled in parallel to a nonlinear rate-sensitive dashpot. Dependence of the time constant, τ_e, on the pressure time derivative was included because the wall viscosity coefficient decreased with the rate of change of the applied strain (4).

A similar differential equation was used to model the dynamics of the myogenic constriction

$$d_m(t) = \frac{1}{\tau_{mo}} (\bar{d}_m(p_d) - d_m), \text{ with } p_d = p(t - t_d) \tag{5}$$

The delayed pressure, p_d, was introduced because the active response to a step-wise arterial pressure change started after a latency period, t_d (10,14). This delay reflected the time needed for the electrochemical transductions and actuations.

Parameters τ_{eo}, μ, τ_{mo} and t_d (Table 1) were assigned to achieve the best fit between experimental (8,10) and model responses to a step-wise luminal pressure change (Fig. 2).

Arteriolar Hemodynamics. The pressure drop across a segment of arteriole mainly was a result of the energy loss caused by the blood viscosity, whereas the capacitive effect as a result of vessel volume changes was negligible. As a consequence, the hemodynamics of an arteriolar branch was modeled by a lumped hydraulic resistance. Myogenic changes in the vessel lumen in response to transmural pressure alterations (Eqs. 1 through 5) gave rise to changes in the hydraulic resistance in accordance with the Hagen-Pouseille law

$$R = \frac{k}{d^4(p)} \tag{6}$$

where the parameter k is proportional to the length of the microvessel segment. The intraluminal pressure p was calculated by averaging the pressure p_p of the inflow section, *i.e.*, the section in which the branching occurs, and the pressure p_d in the outflow section in which a new branch rises:

$$p = p_p + \xi(p_d - p_p) \tag{7}$$

The weighting factor ξ makes it possible to move the average value from the proximal section (ξ = 0) to the distal one (ξ = 1).

Mathematical Model of the Microvessel Network

The anatomical organization of the peripheral vascular bed has a complex topological design that is difficult to reproduce closely. To simplify the analysis, arterioles that branch from a common parent artery were considered as resistances arranged in parallel; therefore, they were lumped in a single equivalent resistance. Moreover, ne-

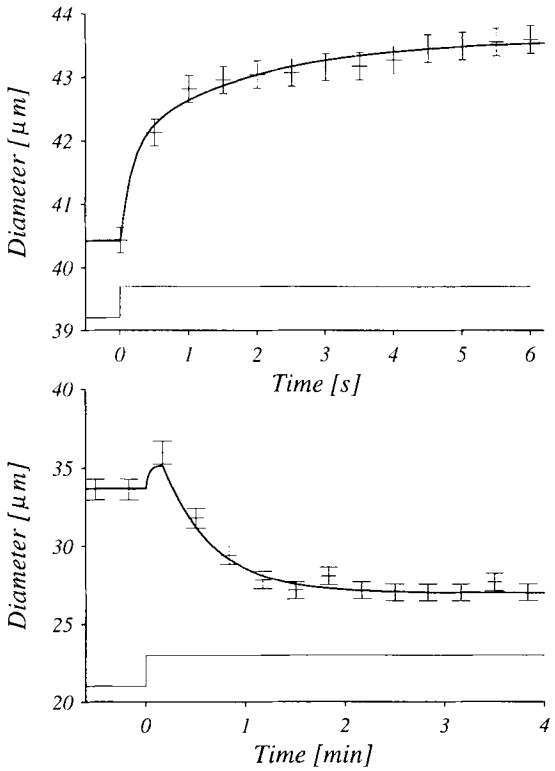

FIGURE 2. Time pattern of a second order arteriole diameter measured by Davis and Sikes (10) in the hamster cheek pouch in response to a step-wise intraluminal pressure change, performed in a purely elastic state (upper panel) and after physiological activation of vascular smooth muscle (lower panel). Bars indicate experimental standard errors. Solid lines represent model simulations, obtained by Eqs. 4 and 5, parameter values are shown in the first column of Table 1.

glecting the anastomoses and limiting the analysis to a single level of branching corresponding to the terminal portion of the arteriolar vascular bed, the network was schematized as shown in Fig. 3.

Proximal arterial circulation was simulated through a resistance-compliance divider. The compliance C was included because small arteries have a prevalent capacitive effect. The variations of the resistance R_a caused by the vessel diameter changes were negligible with respect to those of the downstream vessels, thus, the value of this resistance was maintained constant. The resistance R_i (Fig. 3) simulates the series of the first, second, and third order arterioles (*i.e.*, microvessels with diameter ranging from 50 to 20 μm). These vessels exhibited an evident myogenic activity, and as a result, their resistance, R_i, was regulated according to Eqs. 1 through 6. Parameter values of the myogenic control are those listed in the Table 1. To simulate the effects of the terminal arterioles, three distinct branches were derived. The resistances R_s, R_m, and R_l represent arterioles of the fourth order, *i.e.*, vessels with diameters ranging from 20 to 5 μm. Because vessels of this order show evident myogenic reactivity, these resistances also were regulated. The characteristics of the myogenic control were assumed to be equal for all the three resistances, with just a mild difference in the time delay (Table 1). Moreover, the parameter k of Eq. 6 was assigned a different value, to simulate an asymmetric network with vessels differing in length. In particular, R_s is the shortest branch and R_l is the longest. Each branch was terminated in a resistance R_c, which lumps together the resistive effects of the precapillary and postcapillary circulation. Vessels of these orders do not exhibit myogenic activity, and, so, the resistance R_c was kept constant. The postcapillary circulation was simulated by the resistance R_v closed on the venular pressure P_v.

The value of resistances was assigned (Table 2) to reproduce the hydrostatic pressure profile in the hamster

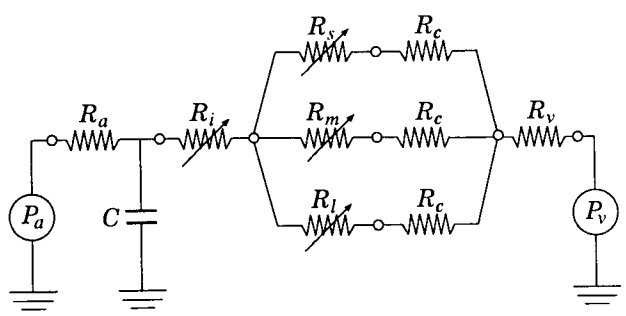

FIGURE 3. Electric analogous of the simulated microvascular network. R_a and C represent hydraulic resistance and compliance of upstream small arteries. R_i, R_s, R_m, and R_l hydraulic resistances of a common parent arteriole and of three terminal arteriolar branches, respectively; R_c and R_v hydraulic resistances of the capillary and postcapillary (venular) circulation; P_a arterial pressure; P_v venous pressure.

TABLE 2.

R_a (dyn s cm^{-5})	3×10^{9}
C (cm^5 dyn^{-1})	1.4×10^{-9}
R_i^* (dyn s cm^{-5})	1.7×10^{10}
R_s^* (dyn s cm^{-5})	2.6×10^{11}
R_m^* (dyn s cm^{-5})	3.7×10^{11}
R_l^* (dyn s cm^{-5})	6.2×10^{11}
R_c (dyn s cm^{-5})	8.5×10^{10}
R_v (dyn s cm^{-5})	1.2×10^{10}
P_v (mm Hg)	8

*At 40 mm Hg.

cheek pouch circulation (9). The venular pressure P_v was settled at 8 mm Hg and was the same throughout each simulation, whereas the arterial pressure level P_a was varied within the range 60–150 mm Hg to evaluate its influence on the system behavior.

RESULTS

A preliminary analysis of the stability of the model equilibrium conditions was performed to assert that the presence of a latency period in the myogenic response was necessary to induce self-sustained microvascular oscillations. In fact, when time delays of all the controlled branches are null, the steady-state of the whole network was structurally stable with respect to each physiological level of the arterial pressure. By giving a value other than zero to the time delay of the myogenic reflex in the resistance R_s only, we were able to make a preliminary examination of the oscillatory behavior of a single arteriole, excluding the interaction with self-sustained oscillations propagating from other branches. Under this particular condition, the influence of the intraluminal pressure, p, (Eq. 7) was evaluated. The arteriole oscillates only when its intraluminal pressure is within a specific range. In fact, in the pressure-diameter characteristic there are two pressure levels, which correspond to two Hopf supercritical bifurcations (23), marking the boundaries between a vasomotion region, characterized by self-sustained vessel oscillations, and low pressure or high pressure regions in which the vessel is apparently inert (Fig. 4). When the intraluminal pressure is settled in these two regions, vessel oscillations are damped out and the diameter sets to a stable equilibrium condition. When the pressure is in the vasomotion region, the steady-condition is unstable and autooscillation occurs. The frequency of this oscillation is strongly affected by the time delay of the myogenic control. We have chosen the value of this parameter within a physiological range (10,14). The frequency of the oscillation emerging from the Hopf bifurcation was equal to 9 cpm, which is a typical low-frequency value for arterioles with diameter similar to that of the simulated vessel R_s (7).

After these preliminar simulations, the myogenic time delay was included in all branches (Table 1) to study how

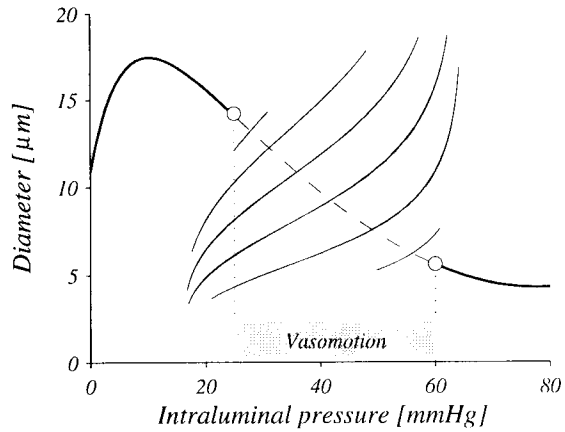

FIGURE 4. Stable and unstable equilibrium conditions on the active pressure-diameter relationship of a terminal arteriole (segment R_s of Fig. 3). Solid bold line represents stable equilibrium points; dashed line represents unstable equilibrium points, around which self-sustained oscillations develop; circles represent supercritical Hopf bifurcations occurring at intraluminal pressure values of approximately 25 and 50 mm Hg. Trajectories followed by the oscillating vessel at different intaluminal pressure mean levels (Eq. 7) are shown.

the arterial pressure p_a influences the network behavior. As long as the arterial pressure level, P_a, was kept at a constant value lower than 65 mm Hg, pressure and flow in each branch tended asymptotically to a stable equilibrium condition (Fig. 5). In this state, vessel deformations, flow distribution, and pressure profile through the network are determined in accordance with the steady-state characteristics.

When the level of the arterial pressure overcame a value of approximately 63 mm Hg, the model underwent a supercritical Hopf bifurcation (Fig. 5). The equilibrium

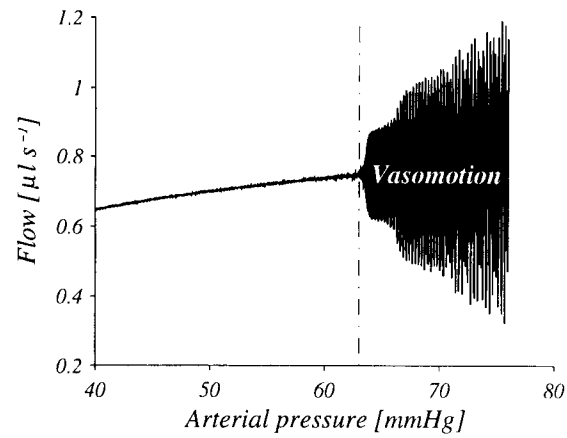

FIGURE 5. Bifurcation diagram showing the emergence of oscillations in blood flow when the arterial pressure level is increased. At arterial pressure levels below 63 mm Hg, network exhibits a stable equilibrium condition with no oscillations; at approximately 63 mm Hg, a Hopf bifurcation occurs, and a self-sustained oscillation appears. Flow was evaluated at the level of the parent arteriole (segment R_i in Fig. 3).

condition became an unstable focus, the arteriolar branches R_s starts to oscillate (Fig. 6), and the system trajectories converge on a limit cycle (Fig.7). Because the network is asymmetric, each branch was characterized by a different intraluminal pressure: R_s was expected to have the highest intraluminal pressure, being the less resistive branch, whereas R_l was expected to have the lowest pressure, being the longest. As long as the arterial pressure level P_a was within the range of 63 to 70 mm Hg, only the branch R_s had a luminal pressure within the vasomotion region, whereas the luminal pressures of R_m and R_l were below their bifurcation level. In this condition, only the segment R_s exhibited a self-sustained oscillation (Fig. 6). In fact, parent upstream vessel R_i oscillated in phase with the forcing oscillation that took place in R_s. The oscillation of the parent vessel R_i was passive because it was sustained by an oscillation propagating from a distal segment of the network. In contrast, the variations induced on the segments R_m and R_l are inappreciable.

When the arterial pressure level was increased above approximately 70 mm Hg, the luminal pressure of the arteriolar branch R_m went into the vasomotion region, and it also started to autooscillate (Fig. 8). The frequency of this self-sustained oscillation differed from the frequency of R_s, because of a different time delay (Table 1). Under this condition, these two vessels were characterized by

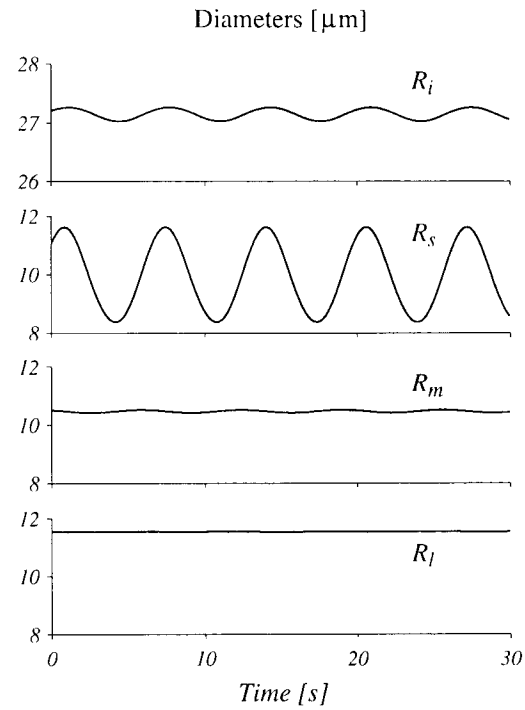

FIGURE 6. Time pattern of inner diameters in the four myogenically active segments of Fig. 3, simulated at an arterial pressure level of 65 mm Hg. The model exhibits periodic dynamics, driven by the self-sustained oscillation occurring in the segment R_s.

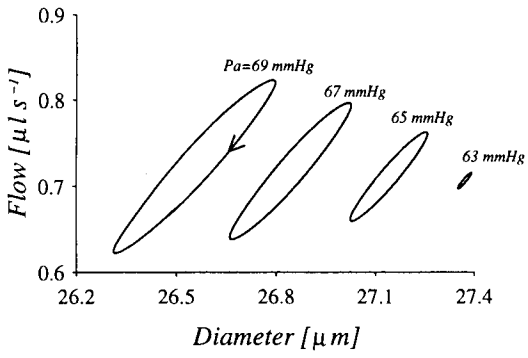

FIGURE 7. Examples of closed periodic trajectories, flow *versus* inner diameter, evaluated with reference to the parent vessel (segment R_i in Fig. 3) at varying arterial pressure levels. Supercritical Hopf bifurcation is recognized by the progressive expanding of limit cycle starting from zero at approximately 60 mm Hg. As a result of myogenic reflex (see Figs. 1 and 4), arterial pressure increases cause the inner diameter to decrease, thereby maintaining constant the mean blood flow.

different rhythms (Fig. 8). Because the two rhythms were incommensurate, phase locking did not occur, and the network behaved quasiperiodically. The critical level of the arterial pressure for which R_m also began to oscillate was a Naimark-Saker bifurcation (6,28): the cycle limit became a saddle cycle, and the system trajectories (Fig. 9), when the transient was extinct, moved on a two-torus

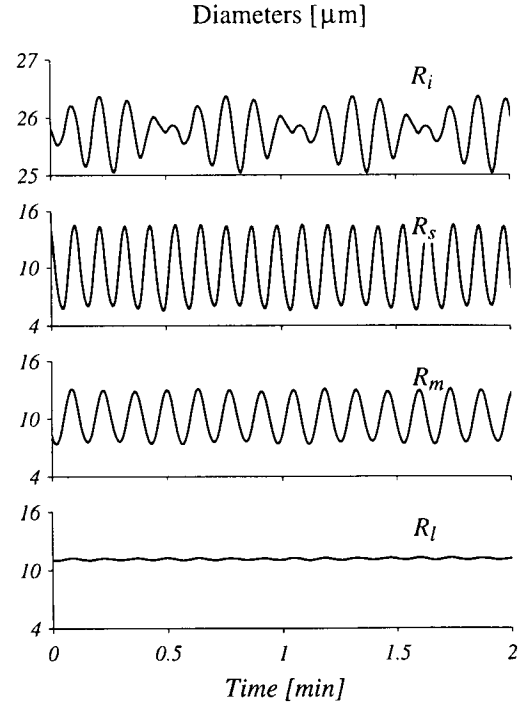

FIGURE 8. Time pattern of the inner diameters in the four myogenically active segments of Fig. 3, for a simulated arterial pressure level of 75 mm Hg. Branches R_s and R_m present self-sustained oscillations with incommensurate frequencies, which force the parent segment R_i to exhibit a quasiperiodic time pattern.

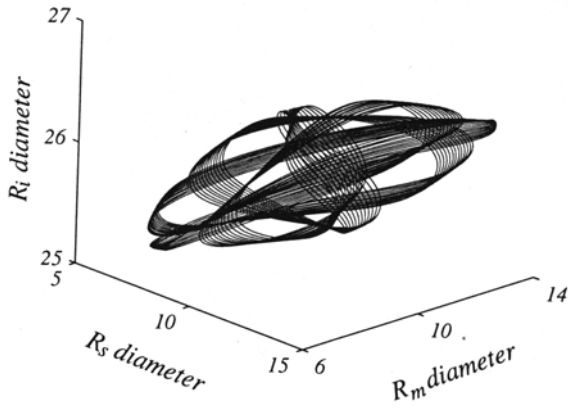

FIGURE 9. Model trajectory in a three-dimensional substate space (inner diameters in branches R_s, R_m, and R_i), computed at an arterial pressure level of 75 mm Hg. Trajectory moves on a two-torus.

(23). The parent vessel R_i still oscillated passively, driven by the downstream oscillations that added together. As is evident from the power spectra (Fig. 10), the parent vessel exhibited a two-periodic oscillation (23), reflecting the two rhythms of the oscillating downstream vessels.

When the arterial pressure was increased above approximately 85 mm Hg, the resistance R_l also began to autooscillate (Fig. 11). In the spectrum of the parent vessel, a new rhythm became evident, the frequency of which was incommensurate with the previous ones (Fig. 12). The new rhythm modified the topology of the attractor: the two-torus became unstable, and a three-torus occurred. Under this condition, because the oscillation was three periodic (23), the time patterns of the parent arteriole diameter and of blood flow were more complex (Fig. 11).

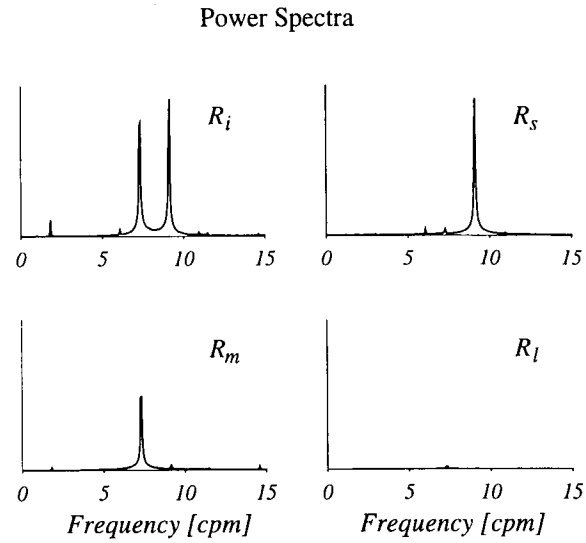

FIGURE 10. Power spectra of the inner diameter oscillations shown in Fig. 8. Two predominant rhythms at incommensurate frequencies appear in the spectrum of the parent vessel R_i, reflecting the self-sustained oscillations occurring in downstream branches R_s and R_m.

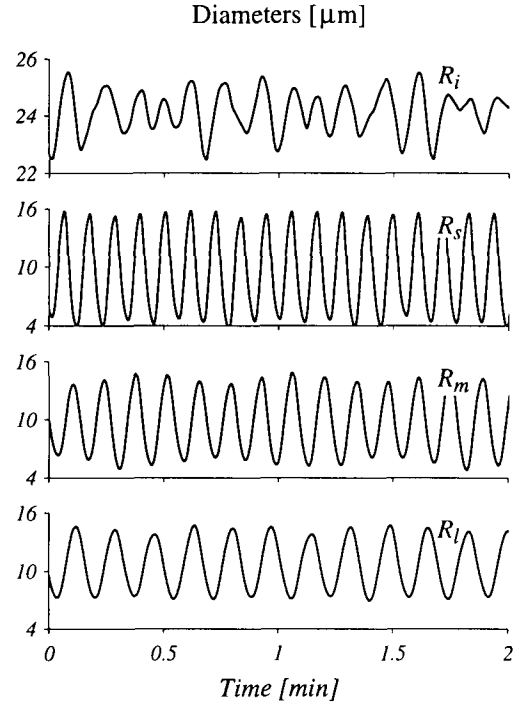

FIGURE 11. Time pattern of the inner diameters at an arterial pressure level of 90 mm Hg. All three terminal branches R_s, R_m, and R_l present a self-sustained oscillation with incommensurate frequencies, thereby causing a quasiperiodic oscillation in parent vessel R_i.

However, the limit set of the Poincaré map (24), as well as of power spectra, confirmed the quasiperiodic nature of the attractor (23).

In the state space, aside from the attracting three-torus, there also were the stable and unstable manifolds of the saddle limit sets (24) springing up from the previous bifurcations. In brief, the presence of saddle invariants in the state space is known to play a significant role in the genesis of chaotic dynamics (28). In fact, at an arterial pressure level of approximately 120 mm Hg, the stable and unstable manifolds of a saddle collided, a homoclinic bifurcation (24,28) occurred, and a strange attractor (23) appeared (Fig. 13). Above this pressure level, the parent upstream vessel R_i behaved chaotically, and pressures, flow, and vessel diameters exhibited irregular, apparently random time fluctuations (Fig. 14) the power spectra of which shows a continuous, broadband component, similar to white noise, with some spikes superimposed on it at frequencies corresponding to the rhythms of the single branches (Fig. 15).

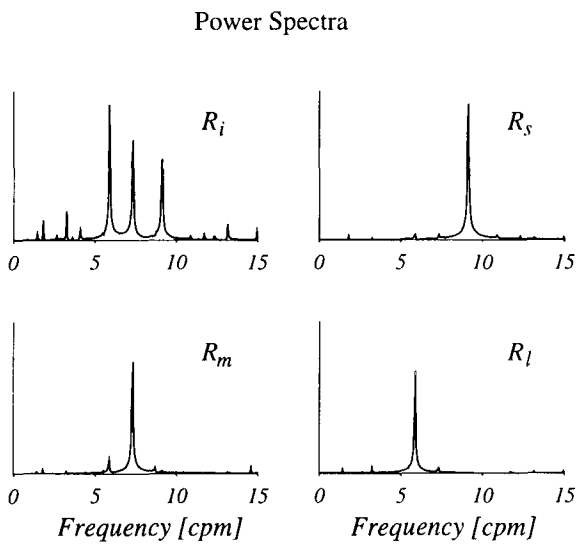

FIGURE 12. Power spectra of inner diameter oscillations shown in Fig. 11. In the spectrum of the parent vessel R_i, three incommensurate rhythms appear with frequencies that characterize the self-sustained oscillations of terminal branches R_s, R_m, and R_l.

Vessel oscillations remained chaotic as long as the arterial pressure level was lower than approximately 150 mm Hg. Overcoming this level, the vessels began to oscillate periodically again, and the network left chaos. Periodic and chaotic windows can be observed alternatively for higher values of the arterial pressure or by changing other model parameters.

The critical levels of the arterial pressure at which bifurcations occurred with a consequent change in system behavior depended on the value assigned to network parameters. When a different value is assigned to one of the model parameters, the bifurcation pressure levels changed, and new kinds of behavior became possible. For example, by increasing the resistance R_i of the parent vessel, intraluminal pressure in the downstream branches was decreased, leaving the vasomotion region. At the same time, the intraluminal pressure of the parent vessel increased, entering into its vasomotion region (Fig. 16). Under this condition, the parent vessel forced the entire network and all branches to oscillate synchronously with the same frequency. Because the second harmonic of this oscillation had a frequency near the frequency of the

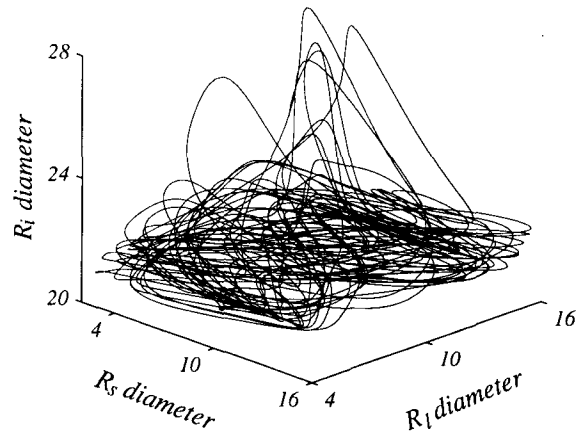

FIGURE 13. Model trajectory in a substate space (inner diameters in branches R_s, R_m, and R_l), computed at an arterial pressure level of 140 mm Hg (transient is deleted). Trajectory moves on a strange attractor.

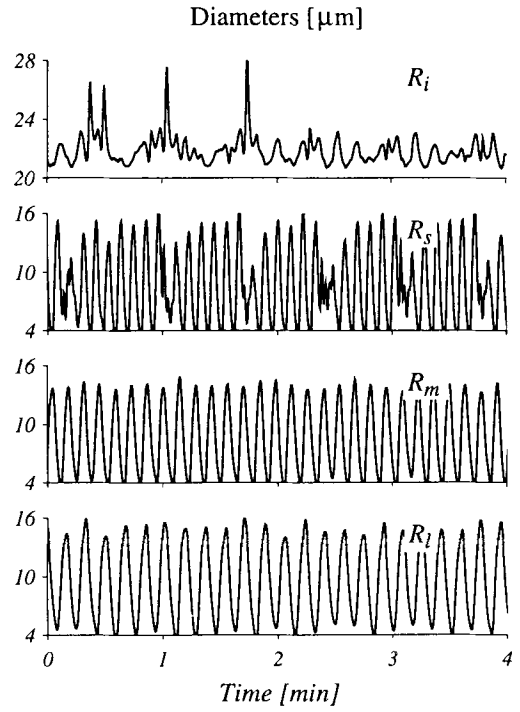

FIGURE 14. Time pattern of the inner diameters for a simulated arterial pressure level of 140 mm Hg. The parent vessel R_i exhibits evident chaotic dynamics with time heterogeneity (correlation dimension Dc = 2.85).

branch R_m, this vessel showed a double rhythm. In this situation, increasing the arterial pressure resulted in a new route toward chaos, similar to the previous one, being found.

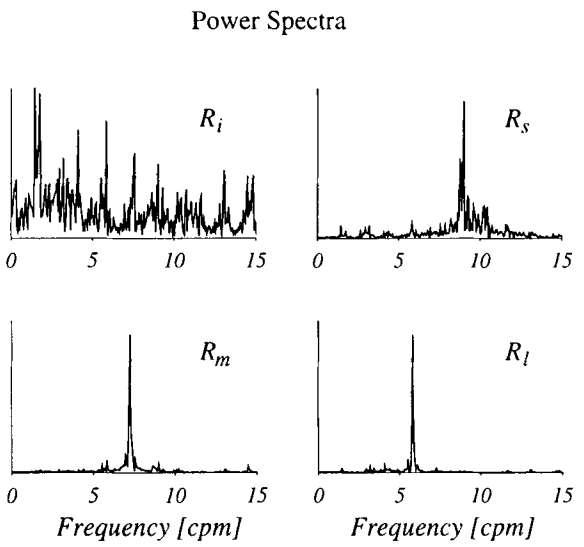

FIGURE 15. Power spectra of the inner diameter oscillations shown in Fig. 14. In the spectrum of the parent vessel, R_i, a broad noise component is superimposed on some predominant rhythms reflecting downstream vessel oscillations.

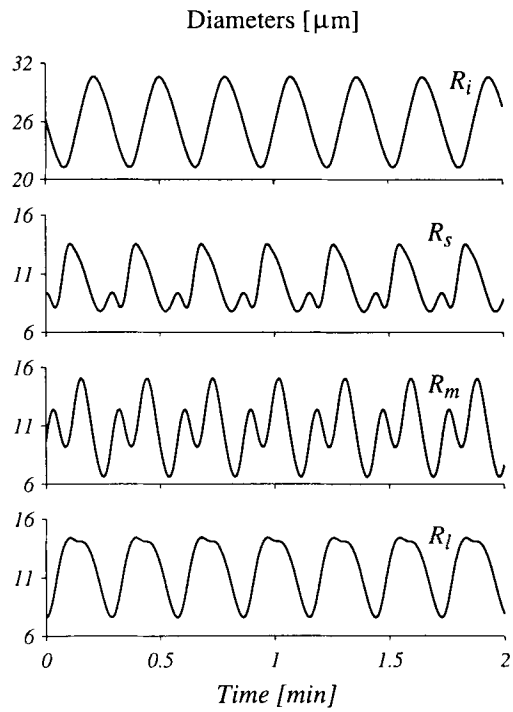

FIGURE 16. Time pattern of the inner diameters in the four myogenically active segments of Fig. 3, for a simulated arterial pressure level of 100 mm Hg, by increasing the length of the parent vessel, R_i. The parent vessel exhibits self-sustained oscillations, which are transmitted to the downstream branches. Branches R_m and R_s show a double rhythm.

DISCUSSION

The presence of a spontaneous rhythmic activity in microvessels has been documented by many investigators in recent years and is a subject of rapidly increasing interest. Nevertheless, biomechanical bases of this phenomenon, the physiological significance, and its possible functional role remain insufficiently understood. To gain a deeper insight into these aspects of vasomotion, we developed a novel mathematical model of arteriolar hemodynamics, which explicitly incorporated microvessel branching in a simplified way. Passive and active mechanisms were included in the biomechanical model of the arteriolar deformation: the passive behavior of the arteriolar wall was similar to that seen in a nonconstricting state, whereas the active mechanism mimicked the myogenic reflex. We have considered only this active mechanism, neglecting other regulatory processes, such as the metabolic and neurogenic ones, to stress the role of the myogenic reflex in the genesis of complex dynamics in the microcirculation. Conflicting results can be found in the physiological literature, as to the strength and the functional importance of the myogenic mechanism. Although some authors (10,17) observed that the myogenic responses was able to induce significant static reductions in microvessel lumen in response to a transmural pressure increase, others (14,21)

found that the myogenic response caused only modest alterations in vessel lumen and resistance. An additional controversy concerns the role of a rate-sensitive component in the active response of arterioles (10,14). This model has been developed on the basis of the experimental results reported by Davis *et al.* (8–10) on the hamster cheek pouch microcirculation. We were able to reproduce these results satisfactorily without needing to include an active rate-dependent component, and, through this model, low-frequency self-sustained arteriolar oscillations were obtained. However, as demonstrated in a previous work (29), oscillations also may be produced by assuming a weaker static myogenic response but including an effective rate-dependent component.

Microvessel oscillations occur when the luminal pressure is within a specific range and, in particular, when the equilibrium point lies on the pressure-diameter characteristic in the region with negative slope. This result agrees with the analysis by Achakri *et al.* (1), thereby indicating that a necessary condition for the diameter oscillations in muscular arteries is the presence of a negative slope in the pressure-diameter relationship. Under this condition, the myogenic control operated as a negative feedback, which, in the presence of pure time delay, could induce instability and the occurrence of self-sustained oscillations. The amplitude of vessel oscillations depended on the intraluminal pressure level (Fig. 4), as occurs in real systems in which vasomotion changes owing to pressure perturbation (22,26). In the model, larger oscillations develop at the points at which the static characteristic has the highest gain (Fig. 4). This result agreed with the experimental observation that vasomotion amplitude tended to be maximal near microvascular branching, where the smooth muscle cells were more active and the myogenic gain was higher (25,19).

On the basis of the observation that some points of the microcirculation exhibited a pronounced synchronous vasomotor activity that drove the entire vessel oscillations, some authors suggested that vasomotion might be coordinated by local vascular pacemakers (7,25). Results obtained in this study suggest an alternative explanation for this phenomenon. According to the model, when the luminal pressure of an arteriole lies within the vasomotion region, the vessel oscillated with a stable and precise frequency. Moreover, this oscillation may force other inert branches (*i.e.*, branches in which the lumen pressure is outside of the vasomotion region) to oscillate synchronously. From this point of view, vasomotion may appear as a forced oscillation, without the need for supposing the existence of local vascular pacemakers.

Simulation results indicate that the myogenic mechanism may cause a variety of oscillatory patterns in a simple arteriolar network, including not only periodic, but also quasiperiodic and chaotic, fluctuations. Each single myogenically, active microvessel (*i.e.*, the resistances R_i, R_s, R_m, and R_l of Fig. 3) may constitute an autonomous oscillator and, because of the network asymmetry, such individual oscillators exhibit disparate characteristics, both as to the frequency and the amplitude of their oscillations. Asymmetry in real microvascular networks may be caused by a multitude of factors, such as differences in length, vessel lumen, or the level of the smooth muscle activity (8). However, the existence of some kind of asymmetry in the network branches, either in the geometry or in the myogenic response, does not seem to be essential for a complex behavior. In fact, simulations performed by giving the same values to the parameters of segments R_s, R_l, and R_m indicated that routes toward chaos can be observed even in a symmetrical network.

In the model, different oscillators interplay through changes in their intravascular pressure. Mathematical theories of coupled nonlinear oscillators (2) suggested that, when the amplitude and the frequency of the oscillators were varied, several different coupling modes became evident. In this study, we have focused attention on the effect of changing systemic arterial pressure, and, because this perturbation modifies luminal pressure in the arteriolar segments, it influences the coupling among the oscillators. We can roughly distinguish between three distinct behaviors. When arterial pressure is sufficiently low, only one segment can actively autooscillate with its intrinsic period, whereas other segments oscillate passively after the forced changes in their intravascular pressure (Fig. 6). When the arterial pressure is increased, other segments cross their bifurcation point, and start to autooscillate. As long as the changes in intravascular pressure are modest, then the coupling strength is small, and one can observe either periodic oscillations in the overall system, if there is a stable entrainment among the oscillators or quasiperiodic fluctuations, and if the individual oscillators maintain incommensurate frequencies. Finally, when the coupling strength among the oscillators becomes high, for instance as a result of an increase in intravascular pressure, one can observe a global bifurcation that destroys the quasiperiodic system behavior and leads to chaotic dynamics.

In accordance with recent experimental data (22,16, 26,27), previous results suggested that changes in arterial pressure and, thus, in perfusion pressure played a critical role in the vessel diameter oscillations. This finding has an important implication on the peripheral autoregulation. In fact, because of nonlinearities, perfusion pressure may significantly influence through vasomotion the effective hydraulic resistance and then take part in the control of local blood flow.

According to the physiological literature (7), the model predicts that vessels of the same order, located in a contiguous area of the microcirculation, may exhibit different kind of behavior. For instance, as shown in Fig. 8, vessels

of the same order may oscillate with different frequencies and comparable amplitude (R_s and R_m) or with the same frequency and a considerably different amplitude (R_m and R_l). Moreover, the model also predicted periodic and aperiodic network oscillations that may be either synchronous or without apparent time correlation (Fig. 14). Aperiodic vasomotion has been observed, among others, in the bat wing (20), hamster skin fold (7), rabbit tenuissimus muscle (22,19,27) and rabbit ear (15). Spontaneous blood flow fluctuations also have been documented in human skin through the Doppler laser technique (25). The power spectra, computed either with the fast Fourier transform (FFT) algorithm or with autoregressive models, sometimes consisted of a few spikes at incommensurate frequencies typical of quasiperiodic dynamics (18); more often, however, they exhibited a noise-like component, which suggests the existence of deterministic chaos (7,16).

Vessel oscillation synchronization predicted by the model originates from the myogenic mechanism action and is limited to contiguous microvessels interplaying through their intravascular pressure changes. Extended synchronization over a wider microvessel area, as observed in experimental studies (25), could be induced by central autonomic control, an aspect that was not considered in this study.

For the sake of brevity, we have not included a deep quantitative analysis of chaotic dynamics in this study, however, both the sensitive dependence on the initial condition and the fractal dimension of the Poincaré map (23) of the strange attractor were verified. The model achieved chaos by following a classic route, as in the Ruelle-Takens-Newhouse scenario (6): by changing the value of a model parameter, in our case, by increasing the arterial pressure level, an equilibrium condition was made to lose its stability and, through a supercritical Hopf bifurcation (24), a stable limit cycle was born, and the system oscillated periodically. An addition increase in the parameter value caused the system to cross a Naimark-Sacker bifurcation (6): the cycle limit became unstable, a stable torus occurred, and the system exhibited a quasiperiodic time evolution. Finally, through a global bifurcation, in particular, a homoclinic explosion (28), the torus lost its stability, a strange attractor appeared, and the system evolved chaotically.

The hypothesis that microvessels may present some aspects of chaotic behavior recently was formulated by some authors (15,16). In particular, Griffith and Edwards observed that perfusion pressure in the rabbit ear alternated intervals with nearly periodic oscillations and intervals with more irregular fluctuations, and that the oscillatory pattern varied significantly in response to the same perturbation. The latter finding was considered an example of the inherent unpredictability of chaotic dynamics. Intaglietta and Breit (16), starting from flow velocity oscillations revealed by Doppler laser measurements, reconstructed a strange attractor in a phase plane with the method of the delay map. During hypotensive hemorrhage the strange attractor collapsed into a single point, thereby demonstrating that complex basal fluctuations are shifted by this perturbation into a periodic rhythm.

One recent hypothesis (12) suggested that signal variability observed in physiological systems is evidence of a chaotic behavior. According to this hypothesis, the dynamics of several physiological systems are governed by the superimposition of many simultaneously operative control actions, and, owing to competitive mechanisms, the main quantities exhibit an apparently random evolution. The presence of more regular dynamics is a consequence of abnormal or pathological conditions, associated with the severe impairment of some control mechanisms. Following this hypothesis, the chaotic behavior in the microvessels has been considered (16) as the result of different, active mechanisms, among others, the action of the smooth-muscle pacemaker, the myogenic reflex, the release of vasoactive substances, etc., which compete to regulate the vessel lumen. When one of these mechanisms became dominant, the transition from chaos to periodicity occurred, whereas, when no predominance was possible, the network behaved chaotically. The results of our work, however, suggest a different explanation. Indeed, in our model, a single control mechanism was able to produce a wealth of different patterns, all observed in microvascular beds, (ranging from periodic to quasiperiodic to chaotic, and the passage from one to the next was just a consequence of modest perturbations in an input quantity or in a parameter, not necessarily associated with a pathological condition or an intrinsic alteration in the microvascular bed.

CONCLUSIONS

This study notes that the nonlinearity that characterizes myogenic control may be the cause of the complex dynamics that may be observed in microcirculation. Considering physiological levels of the arterial pressure, a large variety of time patterns ranging from steady-state to irregular, aperiodic oscillations were reproduced by means of a mathematical model of an arteriolar network. Despite its simplicity, the model permits a deeper understanding of various experimental observations that sometimes seem contradictory. In particular, sensitivity of simulation results to the model parameter changes may be the interpretative key to explaining the different kinds of behavior observed in microcirculation studies. Moreover, the apparently random time fluctuations characterizing vasomotion phenomena are explained as a consequence of chaotic dynamics.

REFERENCES

1. Achakri, H., A. Rachev, N. Stergiopulos, and J. J. Meister. A theoretical investigation of low frequency diameter oscillations of muscular arteries. *Ann. Biomed. Eng.* 22:253–263, 1994.
2. Arnold, V. I. *Geometrical Methods in the Theory of Ordinary Differential Equations*. New York: Springer-Verlag, 1993.
3. Bayliss, W. M. On the local reaction of the arterial wall to changes of the internal pressure. *J. Physiol. Lond.* 28:220–231, 1902.
4. Bergel, D. H. The dynamic elastic properties of the arterial wall. *J. Physiol.* 156:458–469, 1961.
5. Burrows, M. E., and P. C. Jonhson. Diameter, wall tension and flow in mesenteric arterioles during autoregulation. *Am. J. Physiol.* 241(10):H829–H837, 1981.
6. Casti, J. L. *Alternate Realities: Mathematical Models of Nature and Man*. New York: John Wiley & Sons, 1989, pp. 253–280.
7. Colantuoni, A., S. Bertuglia, and M. Intaglietta. Quantitation of rhythmic diameter changes in arterial microcirculation. *Am. J. Physiol.* 246(15):H508–H517, 1984.
8. Davis, M. J. Myogenic response gradient in an arteriolar network. *Am. J. Physiol.* 264(33):H2168–H2179, 1993.
9. Davis, M. J., P. N. Ferrer, and R. W. Gore. Vascular anatomy and hydrostatic pressure profile in the hamster cheek pouch. *Am. J. Physiol.* 250(19):H291–H303, 1986.
10. Davis, M. J., and P. J. Sikes. Myogenic responses of isolated arterioles: test for a rate-sensitive mechanism. *Am. J. Physiol.* 259(28):H1890–H1900, 1990.
11. Fung, Y. C. *Biomechanics: Mechanical Properties of Living Tissues*. New York, Berlin: Springer-Verlag, 1981, pp. 41–50.
12. Goldberger, A. L., D. R. Rigney, and B. J. West. Chaos and fractals in human physiology. *Scientific American* 262: 43–49, 1990.
13. Gonzales Fernandez, J. M., and B. Ermentrout. On the origin and dynamics of the vasomotion of small arteries. *Math. Biosci.* 119(2):127–167, 1994.
14. Grande, P. O., P. Borgstrom, and S. Mellander. On the nature of basal vascular tone in cat skeletal muscle and its dependence on transmural pressure stimuli. *Acta Physiol. Scand.* 107:365–376, 1979.
15. Griffith, T. M., and D. H. Edwards. Mechanisms underlying chaotic vasomotion in isolated resistance arteries: roles of calcium and EDRF. *Biorheology* 30:333–347, 1993.
16. Intaglietta, M., and G. A. Breit. Chaos and microcirculatory control. In: *Capillary Functions and White Cell Interaction*, edited by H. Messmer, Prog. Appl. Microcirc. 18. Basel, Switzerland: S. Karger, 1991, pp. 22–32.
17. Johnson, P. C., and M. Intaglietta. Contributions of pressure and flow sensitivity to autoregulation in mesenteric arterioles. *Am. J. Physiol.* 231(6):1686–1698, 1976.
18. Meyer, J. U., and M. Intaglietta. Measurement of the dynamics of arteriolar diameter. *Ann. Biomed. Eng.* 14:109–117, 1986.
19. Meyer, J. U., L. Lindbom, L., and M. Intaglietta. Coordinated diameter oscillations at arteriolar bifurcations in skeletal muscle. *Am. J. Physiol.* 253(22):H568–H573, 1987.
20. Nicoll, P. A., and R. L. Webb. Vascular pattern and active vasomotion as determiners of flow trough minute vessels. *Angiology* 38:291–308, 1955.
21. Osol, G., and W. Halpern. Myogenic properties of cerebral blood vessels from ormotensive rats. *Am. J. Physiol.* 249(18):H914–H921, 1985.
22. Oude Vrielink, H. H. E., D. W. Slaaf, G. J. Tangelder, and R. S. Reneman. Changes in vasomotion pattern and local arteriolar resistance during stepwise pressure reduction. *Pflügers Arch.* 414:571–578, 1989.
23. Parker, T. S., and L. O. Chuas. *Practical Numerical Algorithms for Chaotic Systems*. New York: Springer-Verlag, 1989.
24. Perko, L. *Differential Equations and Dynamical Systems*. New York: Springer-Verlag, 1991.
25. Schechner, J. S., and I. M. Braverman. Synchronous vasomotion in the human cutaneous microvasculature provides evidence for central modulation. *Microvasc. Res.* 44:27–32, 1992.
26. Schmidt, J. A., M. Intaglietta, and P. Borgstrom. Periodic hemodynamics in skeletal muscle during local arterial pressure reduction. *J. Appl. Physiol.* 73(3):1077–1083, 1992.
27. Slaaf, D. W., G. J. Tangelder, H. C. Teirlinck, and R. S. Reneman. Arteriolar vasomotion and arterial pressure reduction in rabbit tenuissimus muscle. *Microvasc. Res.* 33: 71–80, 1987.
28. Sparrow, C. *The Lorenz Equations: Biforcations, Chaos and Strange Attractors*. Berlin, New York: Springer-Verlag, 1982, 27 pp.
29. Ursino, M., and G. Fabbri. Role of the myogenic mechanism in the genesis of microvascular oscillations (vasomotion): analysis with a mathematical model. *Microvasc. Res.* 43:156–177, 1992.
30. Yasmashiro, S. M., D. W. Slaaf, R. S. Reneman, G. J. Tangelder, and J. B. Bassingthwaighte. Fractal analysis of vasomotion. *Ann. NY Acad. Sci.* 591:410–416, 1990.